# Synthesis and evaluation of phase codes for pulse compression radar

*ANTONIO DI VITO - *□ALFONSO FARINA - *GENNARO FEDELE - **•GASPARE GALATI - *FLAVIO A. STUDER
*Selenia S.p.A., Radar Department, Rome - *□University of Naples - *• University of L'Aquila

*SUMMARY*

*The problem of the synthesis of pulse compression radar signals is examined. A family of waveforms suitable for digital compression is identified in digital (or discrete) chirp.*

*Such a code, obtained through sampling and quantisation of known chirp waveforms, has attractive features such as relative insensitivity to frequency shift (Doppler effect) and low sidelobes.*

*Within the digital pulse compression technique, with compression ratio higher than a few tens, digital chirp codes perform better than other codes suggested.*

## List of symbols

| | |
|---|---|
| B | Instantaneous transmission bandwidth |
| $B_{eff}$ | Chirp signal bandwidth |
| C | Compression ratio $C = T \cdot B = T/\tau_c$ |
| $f_i$ | Instantaneous frequency |
| $f_D$ | Doppler frequency |
| K | Weighting factor of chirp instantaneous frequency for sidelobe reduction |
| $K_D$ | Distortion factor |
| M | Number of distinct code phases |
| N | Number of sub-pulses (elements) of the code (for the Frank code N is the number of phases and $N^2$ the number of elements) |
| $n_B$ | Number of bits |
| P/L | Ratio between peak and lobe amplitudes |
| RF | Radio frequency |
| T | Total duration of transmitted code |
| $T_c$ | Sampling period during reception |
| Tg | Group delay |
| $\delta$ | Phase sampling period and element duration |
| $\Delta S/N$ | S/N loss on the peak |
| $\lambda$ | Wavelength |
| $\mu$ | Rate of variation of the (linear) chirp |
| $\tau$ | Delay |
| $\tau_c$ | Compressed pulse duration |
| $\tau_p$ | Time shift of the peak due to the Doppler effect |
| $\chi(\tau, f_D)$ | Ambiguity function |



## 1. Introduction

In modern coherent radar, the use of a transmitter equipped with power amplifier (usually provided with travelling wave tubes) often implies the necessity to exploit the pulse compression technique to satisfy the requirement for high accuracy and discrimination at full range, in spite of the unfavourable ratio between peak and average power.

In long range surveillance radars (range up to 400 ÷ 500 Km), the compression ratio, defined as the ratio of the duration of the transmitted pulse and that of the compressed pulse, is typically in the range of 100, or greater, depending on the required resolution.

A number of factors enable the choice of the transmitted waveform (which, due to available transmitter techniques, must have a rectangular envelope and therefore can only be phase coded). The main factors are:

— duration of the transmitted and compressed pulse,
— compressed signal sidelobes level,
— sensitivity to Doppler effect.

In the following, we make reference to a typical radar, characterized by:

— transmitted pulse duration: 100 $\mu$sec,
— compressed pulse duration: 1 $\mu$sec,
— maximum admissible Doppler frequency: $\pm$ 20 KHz,
— sidelobes level better than that of a maximum duration Barker code,
— digital compression.

These requirements are usually satisfied by a class of S-band radar for the early warning of targets at speeds in excess of Mach 3. In the following, a brief summary of some of the codes used in pulse compression is made before taking digital chirp into detailed examination.

## 2. The Barker code

The Barker code is a Phase Shift Keying (PSK) binary code where only two phase, 0° and 180° are transmitted ($M = 2$). Let T be the total duration of the pulse and $\delta = T/N$ that of the single sub-pulse (that is the element of the phase code) where N is the number of elements of the code. Barker sequences benefit of the fact that if $\chi(\tau, f_D)$ is the ambiguity function, than /1/:

$$\chi(K\delta, 0) = N, \text{ for } K = 0 \tag{1}$$

$$\chi(K\delta, 0) = \pm 1 \text{ or } 0, \text{ for } K = 0$$

This relationship shows how the peak to sidelobe ratio increases with the number of code elements; however, as there are no Barker codes with more than 13 elements, at the best, lobes are 22.3 dB below the peak. In the presence of Doppler shift the code does not have good characteristics. In fig. 1 the loss of signal to noise ratio on the peak:

$$\Delta S/N = \chi(\tau, f_{D_{max}}) / \chi(0,0) = \chi(\tau, f_{D_{max}}) / N \tag{2}$$

is given as a function of the product ($f_D \cdot T$).

From this figure it can be seen how the losses become considerable as ($f_D \cdot T$) increases. If we want to limit such losses to less than 1 dB, the following relation should apply:

$$f_D T \leqslant 0.25 \tag{3}$$

which, in the worst case ($f_D = 20$ KHz) gives:

$$T \leqslant 12.5\ \mu sec \tag{4}$$

Fig. 1 - Peak amplitude of 13 elements Barker code vs. Doppler frequency.

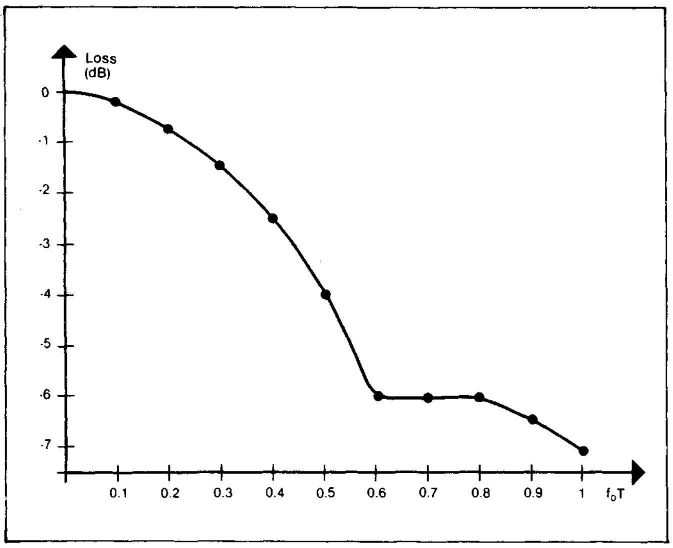


This shows that the coding of long pulses ($T = 80 \div 100\ \mu sec$) cannot take place with this code.

## 3. The Frank code

The polyphase Frank code can be described by the following matrix /1/, /2/:

$$\underline{A} = \begin{bmatrix} 0 & 0 & 0 & 0 & \dots & 0 \\ 0 & 1 & 2 & 3 & \dots & (N-1) \\ 0 & 2 & 4 & 6 & \dots & 2(N-1) \\ & & & & & \\ 0 & \dots & \dots & \dots & \dots & (N-1)^2 \end{bmatrix} \tag{5}$$

where each element is given by the multiplying factor of an elementary phase $\varphi_o = 2\pi p/N$, where p and N are integer prime numbers. Usually p is set equal to 1. If the pulse to be coded is divided into $N^2$ elements, N different phases are obtained. The sequence of the $N^2$ phases can be derived from (5), in fact if Aij is the generic element of the matrix then:

$$\varphi_{ij} = Aij \cdot \varphi_o \tag{6}$$

and the transmitted sequence is built up taking (5) by rows, in other words:

$$e^{j\varphi_{11}}, e^{j\varphi_{12}}, \dots e^{j\varphi_{21}}, \dots e^{j\varphi_{NN}} \tag{7}$$

In order to use this code, the pulse must be divided into a number of elements which is the square of an integer. As an example, for a Frank code of 100 elements there are 10 distinct phases spaced by $2\pi/10$; the time sequence of the phases is given in fig. 2. The compression filter used is the usual delay line where, in the case under examination, 100 delays are needed, each being equal to:

$$\delta = T/N^2 \tag{8}$$

and also 100 complex weights of the type $e^{-j\varphi_{ij}}$.

It is worth mentioning that to generate those weights 100 different complex values (i.e. 200 real values) are not needed, as it is required to generate only 6 distinct values, i.e. 1.0, 0.0, 0.80902, 0.30902, 0.58778, 0.95106 (with sign). Each general term is in fact of the type $\pm a \pm j b$ where a and b take one of the six values given above. Even simpler is the structure of a Frank code with 8 elements, which needs values 1, 0, $\sqrt{2}$.

In absence of Doppler, the ambiguity function gives good characteristics. By normalizing the signal amplitude to 1, it results that:

$$\chi(0,0) = 100$$

$$\chi(K\delta, 0) \leqslant 3.23 \qquad \forall K \tag{9}$$

and therefore the peak to sidelobe ratio is better than 29 dB. However, in the presence of Doppler, this code gives way to considerable losses. The effects can be summarized as follows:

a) For $f_D \cdot T \leqslant 0.5$, a progressive attenuation of the peak $\chi(0, f_D)$ is noted, up to the worst case when $f_D T = 0.5$ where $\chi(0, f_D)/\chi(0,0) = 0.64$ and therefore the loss is 3.92 dB. At the same time, the adjacent lobes increase and when $f_D \cdot T = 0.5$, then:

$$\chi(0, f_D) = \chi(-\delta, f_D) \tag{10}$$

so that the peak to sidelobe ratio is 0 dB. It must also be noted that $\chi(K\delta, f_D)$ is not symmetrical around $\tau = 0$, as is the case for the Barker code.

b) When $0.5 \leqslant f_D T \leqslant\leqslant 1$, the amplitude of the main peak increases and when $f_D T = 1$,

$$\chi(\tau, f_D) \mid_{max} = 97.4$$

However, the peak is shifted by $\delta$, that is $\chi$ has a maximum when $\tau = -\delta$. This means that the range accuracy, in terms of systematic error, is tied to the duration of $\delta$. If $\delta = 1\ \mu$sec, the accuracy is 150 m.

c) When $1 \leqslant f_D T \leqslant 2$, the behaviour observed for $0 \leqslant f_D T \leqslant 1$ is repeated. In figure 3, the loss on the peak is given as a function of $f_D T$:

$$\Delta S/N = \chi(\tau, f_D)_{max} \ / \ \chi(0,0) = \chi(\tau, f_D)_{max} \ / \ N^2$$

From fig. 3, a 4 dB ripple can be appreciated. Furthermore it must be taken into account that the peak shifts in the time domain by $\delta$ each time $f_D T$ increases by 1, so that if $T = 100\ \mu$sec and $N^2 = 100$, in the worst case when $f_D = 20$ kHz, range accuracy is 300 m (and the peak is shifted by $2\delta$).

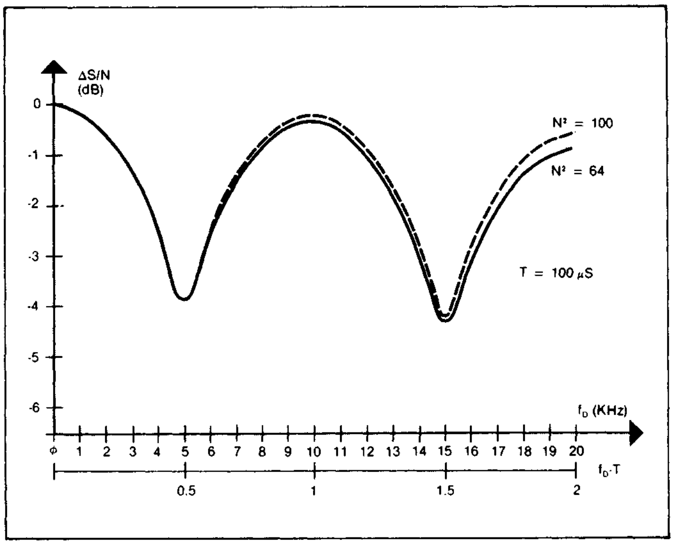


Fig. 3 - Peak amplitude vs. Doppler frequency for Frank codes (100 and 64 elements).

Fig. 2 - Sequence of phase values for a 100 elements Frank code.

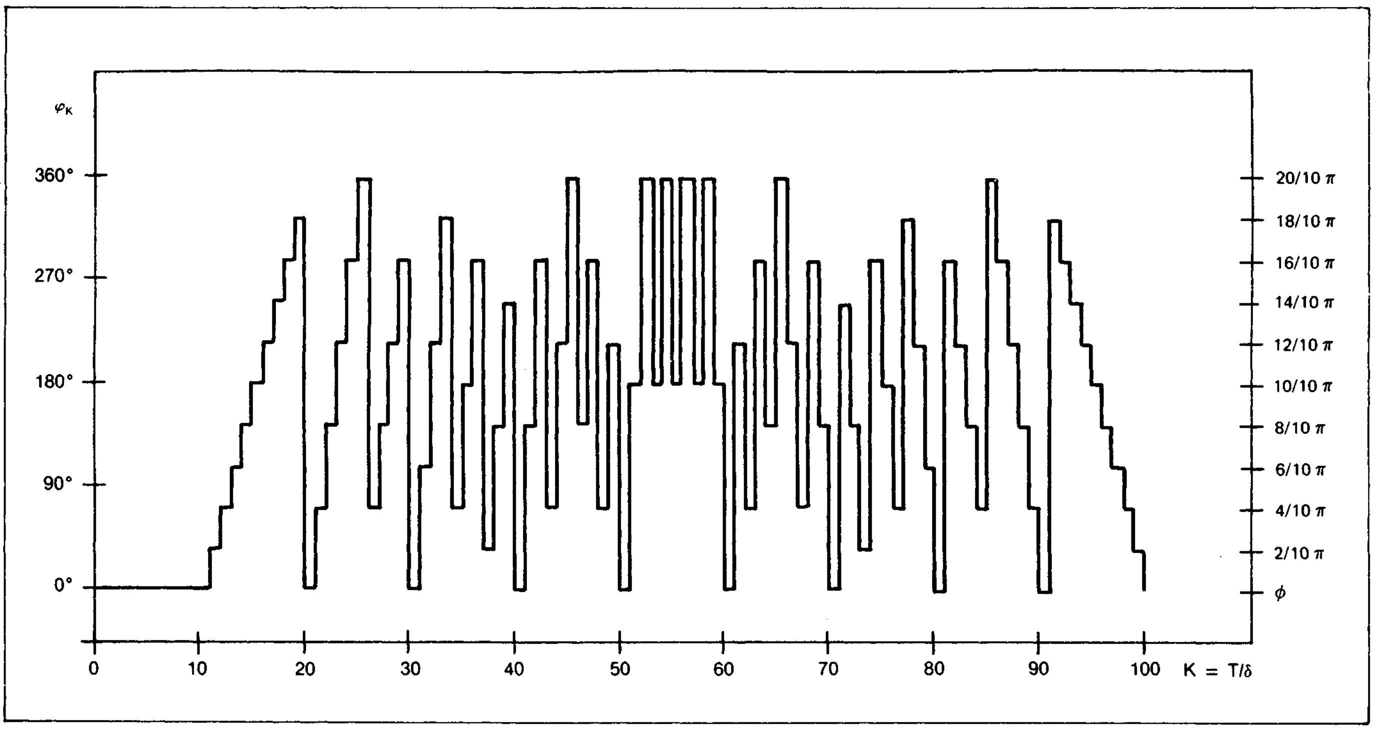

In fig. 4 the variation of the peak-to-highest sidelobe ratio is reported. When $f_D \cdot T = 0.5$ and 1.5, peak and lobe are of equal amplitude although, fortunately, also adjacent. From figs. 3 and 4 it can be seen how in passing from N = 8 to N = 10 with T constant, a slight improvement is gained: increasing N further without increasing the duration T over and above 80 ÷ 100 $\mu$sec gives way to implementation problems in the generation and compression. The analysis performed in /10/ proves incorrect some statements given in /2/. Frank infact, states that the code has a property similar to that of chirp (linear FM modulation). On the contrary, it appears that this code can be used with advantage only when $f_D T \leqslant 0.25$ as in the Barker code. This fact may be explained as follows: the higher the phase variation between the leading edge and the trailing edge of the pulse, the more resistent the code to the Doppler shift. With N = 10, the first sub-pulse has a null relative phase, whereas the last one has a phase $2/N\ \pi\ (N - 1)^2 = 16.2\ \pi$. Correspondingly, there is an associated frequency variation equal to 160 KHz, too small to contrast a Doppler of 20 kHz. Also from this appreciation derives the necessity to increase the number of code elements, but this needs trading off against hardware complexity.

## 4. Frequency modulated pulse

A common technique in pulse compression radars is that of a continuous frequency modulation of the pulse to be transmitted (chirp). Let B be the instantaneous frequency band transmitted and T the pulse duration. It is known /3/ that the response of the compression filter follows, in the case of linear frequency modulation, a

Fig. 4 - Peak-to-sidelobe ratio vs. Doppler frequency for Frank codes (100 and 64 elements).

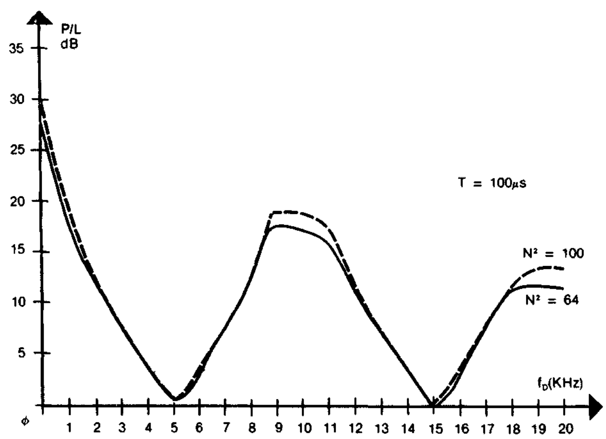


temporal law of the sin x/x type, having a peak value equal to $\sqrt{BT}$ and width equal to 1/B. The main advantage of this waveform is the almost total insensitivity to Doppler, in the sense that the undesired Doppler frequency does not modify the shape of the compressed pulse; in other words, it does not give way to an appreciable increase of sidelobes and the main peak is at the worst attenuated by 1 dB, up to $|f_D\ T| \leq 2$. However, a Doppler shift gives an apparent range variation /5/ due to the time shift of the peak response of the matched filter. The amount of such a shift is a linear function of the ratio $f_D/B$ and therefore such effect can be easily minimized by increasing B, keeping T constant.

To reduce the sidelobe levels from -13.2 dB due to sin x/x to the desired values (-35 ÷ -45 dB) the following techniques can be adopted:

a) use of a nonlinear frequency modulation and a matched filter in reception,

b) use of a linear modulation and a proper filter (not perfectly matched) in reception.

The main characteristics of frequency modulated signals and of the sidelobe reduction techniques are reviewed in sects. 5 and 6. The use of frequency modulated signals implies the use of intermediate frequency analogue techniques for the generation and the compression of a given pulse (Surface Acoustic Wave devices, SAW). However it is possible to derive from such signals some discrete phase codes (i.e. PSK) which approximate analog signals and maintain their main features. These discrete codes are an extension of the biphase codes (Barker type). The analysis and synthesis of such codes is the subject of sects. 7 and 8, where some implementation problems are also discussed.

## 5. Review of frequency modulated signal techniques

"Chirp" is a signal characterized by a rectangular envelope in the time domain and a linear (true chirp) or nonlinear (NLFM) frequency modulation. Chirp compression is achieved by means of a dispersive filter having a group delay which is an appropriate function of frequency. Consider first the case of linear frequency modulation. The transmitted signal is represented as:

$$\begin{cases} s(t) = a(t) \cos(\omega_0 t + {}^1\!/_2\, \mu t^2);\ -T/2 \leq t \leq T/2 \\ s(t) = 0 \quad \text{elsewhere,} \end{cases} \tag{11}$$

where:

T (sec) is the pulse duration;

$\mu$ (rad/sec$^2$) is the rate of change of the angular frequency;

$B \triangleq \mu T$ (rad/sec) is the overall variation of the angular frequency within the pulse duration;

a(t) is the signal amplitude envelope; it is generally rectangular and of unit amplitude within $-T/2 \leq t \leq T/2$.

The mathematical expression of the matched filter impulse response is

$$h(t) = s^*(-t)$$

The output of the matched filter has the following expression /3/:

$$g(t) = \sqrt{BT}\,\frac{\sin \pi Bt}{\pi Bt}\cos \omega_o t \qquad (12)$$

in the absence of Doppler. The presence of a Doppler shift in the echo gives way, at the filter output, to the following phenomena:

1) lowering of the peak
2) time-shift of the peak,
3) ambiguity in the joint estimation of t and $f_D$.

Fig. 5 gives the peak losses and time shift as a function of the Doppler $f_D$ related to the total frequency variation B.

Fig. 6 shows how the output signals $g(t, f_D)$ are distorted due to a Doppler shift of the received signal /4/. It should be noted that the peaks are contained in a triangular envelope, extending from - T to + T, corresponding to the autocorrelation of the envelope a (t) of the input signal.

As for point 3) above, the filter output has a maximum for $2\pi f_D + \mu t = 0$. The time delay $\tau$ of the peak, as a function of $f_D$, is:

$$\tau = \frac{f_D\,T}{B}$$

In the case of perfect matching, the filter output has an envelope of the sin x/x type as given in equation (12).

It can further be shown that for high compression ratios the chirp signal has a flat amplitude spectrum within (-B/2, B/2) and a square law phase spectrum of the type:

$$\theta(f) = 2\,\pi^2\,(f-f_o)^2 / \mu \qquad (13)$$

The corresponding matched filter is therefore a bandpass, centered upon $f_o$, with a group delay which is a linear function of frequency, of opposite slope with

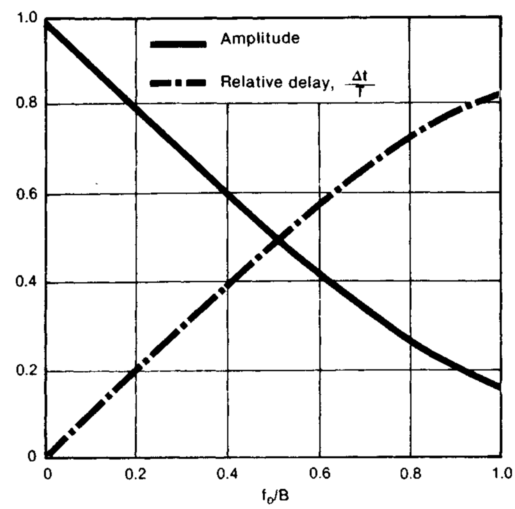


Fig. 5 - Matched-filter-output amplitude and time shift as functions of $f_D/B$ for LFM (chirp) codes.

Fig. 6 - Envelope of linear FM pulse compression matched-filter outputs for different ratios $f_D/B$.

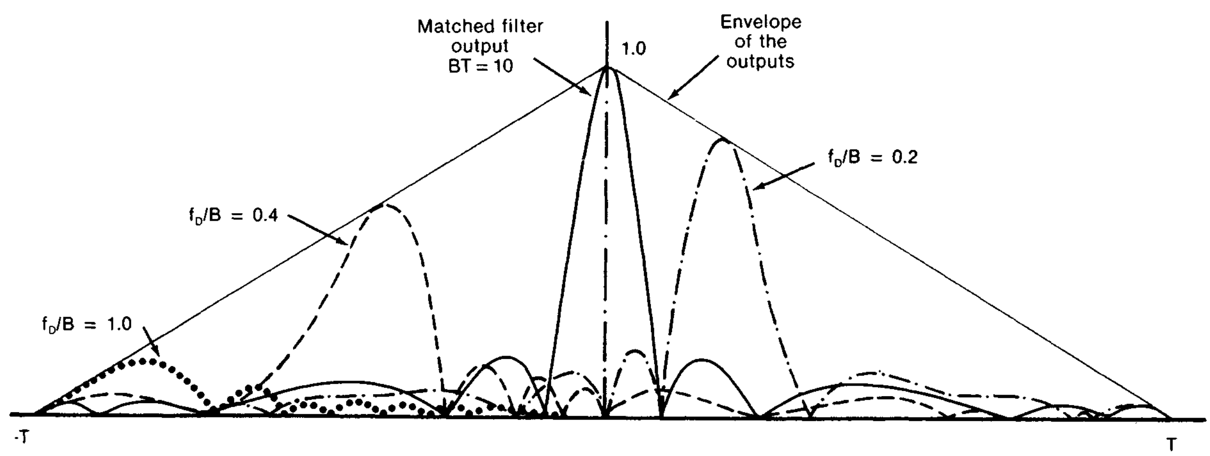

respect to that of the transmitted signal /1, 4/.

The effect of a finite compression ratio on the signal spectrum /1/, /13/, is shown in fig. 7 (C = 60) and fig. 8 (C = 120). As the compression ratio increases, the spectrum approximate all the more a rectangle. Two shortfalls can however be singled out:

- a ripple within the band ± B/2,
- a tail outside the interval ± B/2.

A few notions /1, 3/ relative to nonlinear frequency modulated signals will now be recalled:

- ☐ instantaneous frequency,
- ☐ group delay,
- ☐ stationary-phase principle.

In particular, the stationary-phase principle provides a very simple, although approximate, relationship between the signal frequency spectrum characteristics and its time characteristics, by means of expressions involving only differentials, and not integrals, as is the case of Fourier transforms.

Consider a narrow-band signal s (t):

$$s(t) = a(t)\cos(\omega_0 t + \varphi(t)) \qquad (14)$$

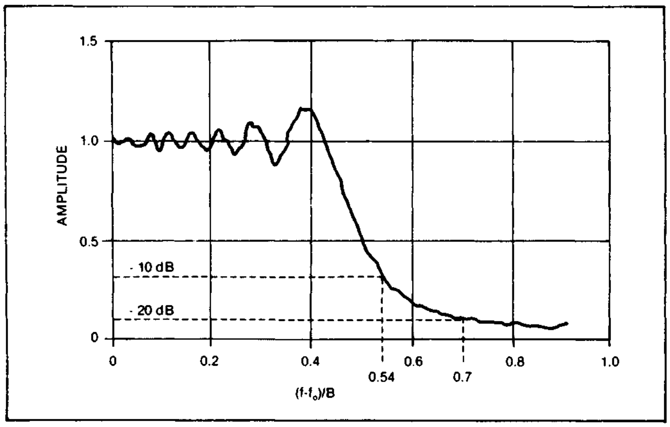


Fig. 7 - Fourier transform of a chirp signal with finite time-bandwidth product (C = 60).

Fig. 8 - Fourier transform of a chirp signal with finite time-bandwidth product (C = 120).

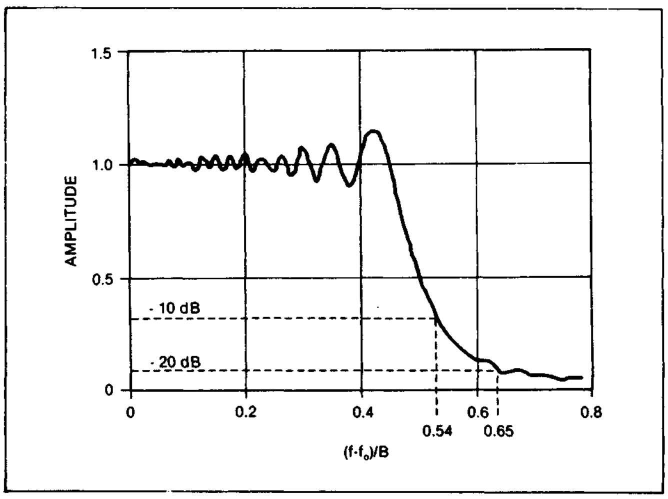


having an envelope a (t) which is usually constant. In this case, it is possible to define an *instantaneous frequency,* (function of time):

$$f_i(t) = \frac{1}{2\pi}\left[\omega_0 + \frac{d}{dt}\varphi(t)\right] \qquad (15)$$

such that the continuous-wave signal cos $(2\pi f_i t)$ approximates the function cos $(2\pi f_0 t + \varphi(t))$ in an interval around t. Further, a *group delay,* (function of frequency) can be defined as follows:

$$\tau_g(f) = -\frac{1}{2\pi}\frac{d\theta(f)}{df} \qquad (16)$$

where $\theta$ (f) is the phase spectrum of s (t).

For each frequency component of the spectrum, $\tau_g$ (f) gives the delay with which such component will be delivered at the output of a filter having $\theta$ (f) (*) as a phase spectrum.

Consider now signals having a group delay which is a monotonous function of f. It follows that the frequency f of the spectrum becomes the instantaneous frequency $f_i$ (t) of the signal at a time instant equal to the group delay. Therefore it can be derived that the instantaneous frequency of a signal and the group delay are inverse functions of each other:

$$\begin{aligned} f_i(t) &= f \quad \text{for } t = \tau_g \\ \tau_g(f) &= t \quad \text{for } f = f_i \end{aligned} \qquad (17)$$

The *stationary-phase principle* /4/ is based upon the following consideration: in the integral relation which defines the Fourier transform of the signal s(t), for each frequency f, the most significant signal contributions are those in an interval around time t where the phase is stationary, i.e.:

$$\frac{d}{dt}(\varphi(t) - 2\pi ft) = 0 \qquad (18)$$

which defines the instantaneous frequency in t. Similarly, in the inverse transform, for each value t, the most significant frequency contributions come from an interval around f where the dual relation holds:

$$\frac{d}{df}(\theta(f) + 2\pi ft) = 0 \qquad (19)$$

which defines the group delay $\tau_g$ (f).

---

(*)In the following it will be assumed for sake of simplicity that $\omega_0 = 0$, therefore: $|s(t)| = a(t)$, and $\angle\, s(t) = \varphi(t)$

We also have that the energy contained in an interval around $\tau_g$ (f) is equal to that in an interval around $f_i$ ($\tau_g$):

$$|s(t)|^2 dt = |S(f)|^2 df, \text{ for } f = f_i \text{ and } t = \tau_g \tag{20}$$

From equations (16-20) the following relevant relationships derive:

$$\left| \frac{d^2}{df^2} \theta(f) \right| = 2\pi \frac{|S(f)|^2}{|s(t)|^2} \tag{21}$$

(which holds in an interval around the instantaneous frequency $f_i$) and:

$$\left| \frac{d^2}{dt^2} \varphi(t) \right| = 2\pi \frac{|s(t)|^2}{|S(f)|^2} \tag{22}$$

(which holds in an interval around $\tau_g$).

The above relationships enable to conveniently design the phase spectrum (i.e. the phase modulation) as a function of the desired time and frequency envelope. In particular, if a signal having an envelope which is rectangular in both time and frequency domains, is to be transmitted then phases $\varphi$ (t) and $\theta$ (f) must be quadratic functions (chirp signal, ref. to equations (11) and (13)).

A further, fundamental relation, which can be derived from the stationary-phase principle, in the case of constant envelope signal (which is the case of the radar pulse) is:

$$\left| \frac{d\tau_g(f)}{df} \right| = c\,|S(f)|^2 \tag{23}$$

relating the group delay to the signal amplitude spectrum ("c" being a constant). This relation may be used to synthesize a NLFM code having sidelobes lower than those of linear chirp (see also /7/).

# 6. Review of methods for sidelobes reduction

It has been shown that a chirp signal has an autocorrelation function given by sin x/x, and the first sidelobe is 13.2 dB below the peak. Furthermore, the close-in sidelobes decrease gradually, by approximately 4 dB for each time interval between two consecutive nulls. Such autocorrelation function behaviour is unacceptable in radar applications, where more than one target is present, giving rise to echoes of different amplitudes.

The optimum receiver for this application is not generally the matched filter. In the practice, however, for simplicity reasons, discrimination problems are faced by using the matched filter in reception and optimizing the waveform so as to keep the mutual interference between targets at acceptable levels. An alternative, used in the practice, is to introduce a mismatch in the receiver. This mismatch must, however, be limited to keep the S/N ratio degradation moderate.

As already recalled in Sect. 4, the methods which can be used to obtain a response with low sidelobes are the following:

1) Weighting in the time domain
2) Weighting in the frequency domain
3) Nonlinear frequency modulation.

Technique 1) correspons to the amplitude modulation of the transmitted signal; as the transmitters used are peak power limited and usually work in saturation, such solution implies a reduction of transmitted power, and therefore a S/N loss. In practice such technique is not used.

The second method for sidelobes reduction exploits the elementary properties of the Fourier tranform. In fact, the transfer function of the receiver is tapered at the band edges. This gives way, in the time domain, to the reduction of the sidelobes, at the expense of a flattening and spreading of the output peak.

The method for sidelobe reduction through receiving filter mismatch is of limited use in the case the radar return has a random Doppler shift. In fact, under the assumption that the transmitted signal has a rectangular spectrum, the mismatched filter output spectrum is a good replica of the filter frequency response and therefore it maintains its sidelobe regularity.

In the presence of a Doppler shifted echo, the output presents an asymmetrical spectrum, with sharp variations at one edge, like the transmitted signal, of which it maintains the high sidelobes.

The technique 2) is then based upon a receiving filter having a properly shaped frequency response to obtain low sidelobes at the output, whereas mismatch losses on the peak are kept at an acceptable level. The shape of the frequency weighting function is designed according to the theory of paired echoes /5/. According to this theory, if the spectrum G (f) of a signal g (t) is modified by modulating it with a cosine law:

$$G_1(f) = G(f)\,[1 + a_n \cos(2\pi n f/B)] \tag{24}$$

the corresponding time signal $g_1$ (t) becomes:

$$g_1(t) = g(t) + \frac{a_n}{2}\,[g(t + nB^{-1}) + g(t - nB^{-1})] \tag{25}$$

This shows that a pair of echoes have been added to g(t), each having the same shape as g(t), but time-shifted and weighted by $a_n$.

An application of this method is reported in Fig. 9, where parameter $F_1$, equal to $a_n/2$, appears. In Fig. (9.a) the function $w_0$ (t) is reported, corresponding to a spectrum having constant amplitude $W_0(f)$. As $W_0$ (f) decays sharply at the band edges, $w_0$ (t) has high sidelobes. In fig. (9.b), on the contrary, it can be seen how by overlaying $W_0$ (f) with an opportune cosine law, the paired echoes produced, are opposite in phase with the first lobes of $w_0(t)$. This produces a lowering of sidelobes and a widening of the main peak.

Setting $F_1 = 0.426$, the so-called Hamming weighting is obtained. The function $W_1$ (f) is similar to the well known weighting function *"Cosine-square with pedestal"*:

$$W(f) = k + (1-k)\cos^2(\pi f/B) \qquad (26)$$

where the amplitude k of the pedestal is related to the parameter $F_1$, as follows

$$k = (1 - 2F_1)/(1 + 2F_1) \qquad (27)$$

Therefore, for a Hamming weighting, a factor $k = 0.08$ is required. As a consequence of the weighting, the sidelobes amplitudes become reduced and the output peak is widened. The magnitude of such variations is given in Fig. 10, where the ratio P/L and peak width between -3 dB points are given as functions of k.

The figure refers to a generalization of (26) where the cosine is raised to a power n. In /1, p. 185/ the equivalence (from the viewpoint of sidelobes structure) between frequency weighting of the received signal and the time weighting of the envelope of the transmitted signal is demonstrated. This equivalence holds only for high compression ratio values.

Technique 3) attempts the synthesis of an NLFM signal, such that the response of its matched filter satisfies the sidelobe requirements. The method for NLFM synthesis is based upon the principle of stationary phase,described in section 5. As the receiver is matched to the signal shape, no mismatch losses, as in methods 1) and 2), take place. However, method 3) suffers from the drawback of peak losses and increase of sidelobes when the received signal has a very high Doppler shift. For an intuitive understanding of this phenomena, one may think that the signal, having a nonlinear frequency coding, can be broken down into a number of chirp signals, each having a different velocity rate $\mu$; the ambiguity function of each chirp will present a ridge in the ($f_D$, t) plane along a line $f_D + \mu t = 0$.

The ambiguity function of the code will result from the superposition of such ridges. These ridges add to each other only in the origin of the plane ($f_D$, t); as the volume under the ambiguity function is constant, the amplitude of each ridge decreases and this corresponds to a greater sensitivity of the code to the Doppler shift.

Let us now describe a method for the synthesis of the

Fig. 9 - Application of paired echoes tecnique (from pages 20, 27 of /5/).

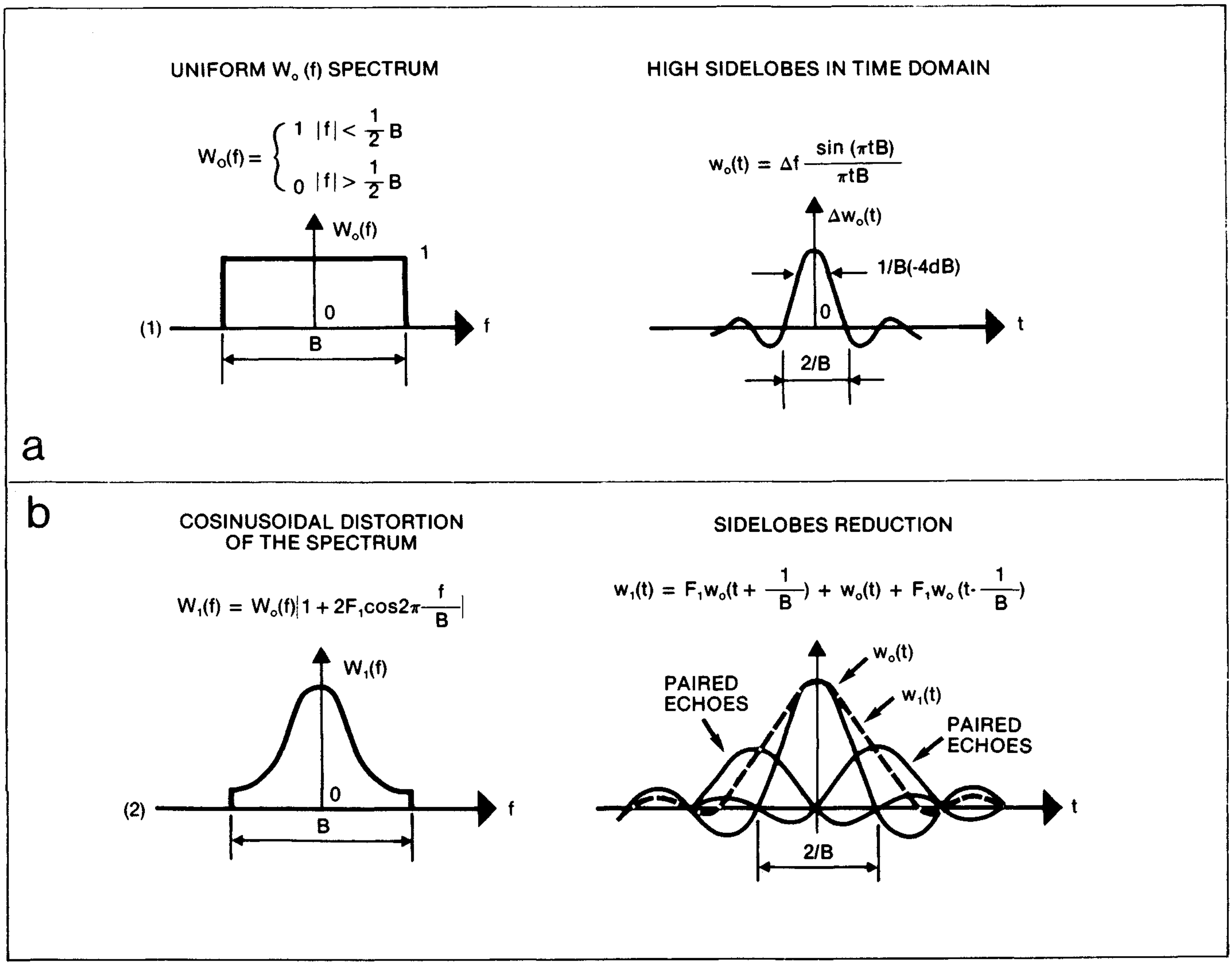

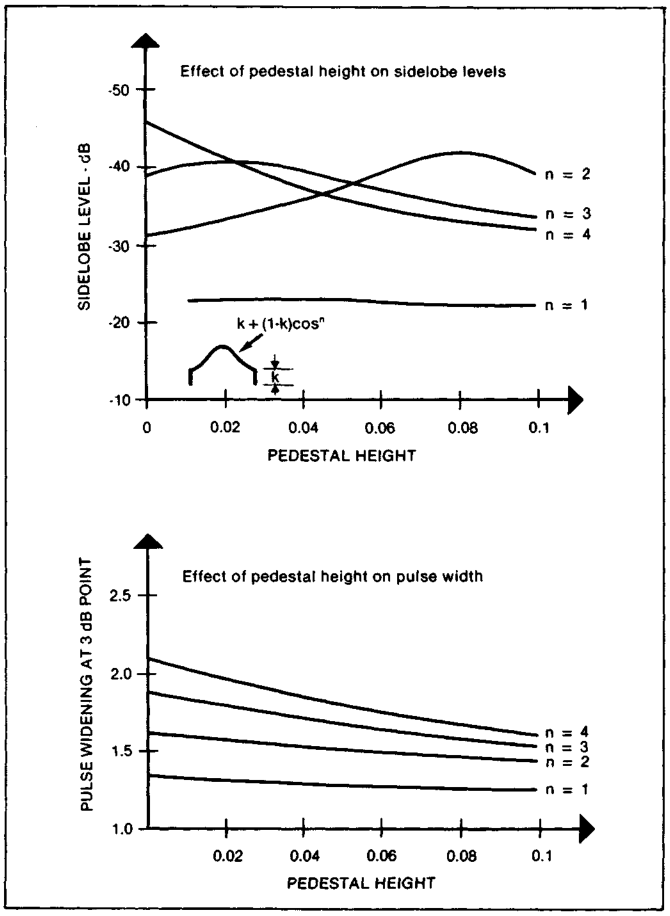


Fig. 10 - Effect of weighting in the frequency domain (from/1/).

NLFM code. A desirable spectrum is defined for the output $|S(f)|^2$ which corresponds to the filter response which would be used in the frequency weighting technique. The weighting function is shared between the expansion and the compression channels; therefore the spectrum of the transmitted signal and the response of the corresponding matched filter may be assumed equal to $|S(f)|$. Such spectrum can be approximated, for high compression ratios, by a suitable modulation law $\tau_g(f)$ (ref equation 23) which is all the more accurate the higher the product band-duration of the rectangular pulse is.

By adopting a cosine square on a pedestal (eq. (26)) law for $|S(f)|^2$, the following expression /7/ can be derived from equation (23) for the group delay:

$$\tau_g(f) = -\frac{T}{2\pi}\left(\frac{f-f_o}{B} + \frac{1-k}{1+k}\sin\frac{f-f_o}{B}\right) \tag{28}$$

which is reported in Fig. 11.

At the expansion filter output, a rectangular pulse is obtained, having an amplitude equal to $|S(f)|$; if the compression channel in reception is matched, the output spectrum is $|S(f)|^2$ as desired ($\cos^2$ on a pedestal) with the required sidelobes level, corresponding to the value chosen for k.

To summarize, we may state that, through the technique presented, it is possible to synthesize a chirp radar signal having the following characteristics:

- low sensitivity to Doppler (like the linear chirp from which it differs by a selected value k, ref figure 11);
- low sidelobes from the matched filter such as for a signal which undergives frequency weighting of the raised cosine type;
- no mismatch losses, because the compression filter is matched to the transmitted signal;
- the parameter k sets the sidelobes level, the main peak width and the sensitivity to Doppler.

In order to accomplish the signal synthesis from equation (28), /7/, the inverse function:

$$f_i(t) = \tau^{-1}_g(f) \tag{29}$$

must be numerically derived.

From this, through integration, the time phase modulation law can be obtained:

$$\varphi(t) = \varphi(t_o - T/2) + \int_{t_o - \frac{T}{2}}^{t} f_i(\tau)\, d\tau \tag{30}$$

The signal obtained has a continuous type of phase modulation. The ensuing section 7 will show how it may be approximated by a polyphase code (PSK), which can be processed by digital techniques.

# 7. Digital chirp code synthesis and performance evaluation

## A) FM CODE SAMPLING

The main requirement set on the code is that of target range resolution, which is related to the -4 dB width $\tau_c$ of the compressed pulse. As $\tau_c$ is a function of band B (frequency modulation shift) dependent upon the selected modulation, the band is fixed. The available peak power

Fig. 11 - Nonlinear frequency modulation (from /7/, p. 74): group delay vs. frequency.

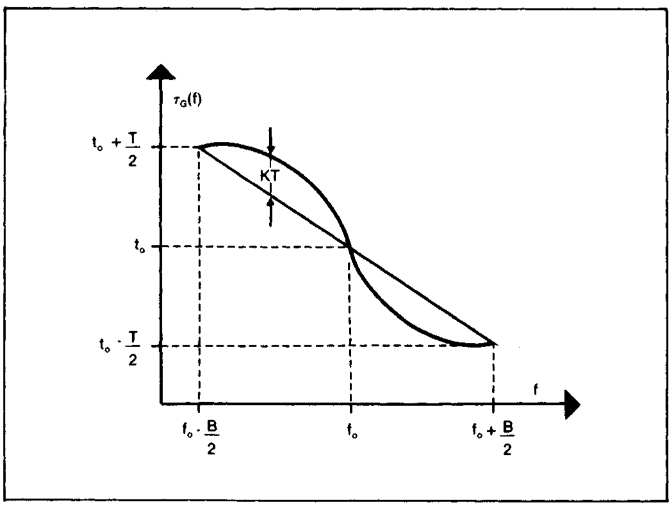

and the energy required to satisfy the range requirement set the duration T of the transmitted pulse: from this the compression ratio value follows: C = BT.

The mathematical notation for a phase modulated signal, in accordance with the parameters determined above, is given by equation (14), where a(t) is equal to unity between -T/2 and + T/2 and is zero elsewhere.

Taken back to base band, the analytic signal s(t) is of the type:

$$s(t) = e^{j\varphi(t)} \tag{31}$$

According to the sampling theorem, such signal can be represented by its samples taken at intervals of width $\delta$ within -T/2 and +T/2

$$s_k = s(k\delta) = e^{j\varphi(k\delta)}, \quad k = 1,2,..N \tag{32}$$

The signal so obtained is a succession (code) of subpulses of same amplitude 1 and duration $\delta$, each having a suitable phase. Therefore starting from an analog frequency modulation a phase modulation, well suited for digital processing of the signal, is obtained. Such a code is denoted by "polyphase code". A constraint in the sampling interval selection is that $1/\delta$ be sufficiently larger than the effective signal bandwidth $B_{eff}$, in which greater part of the signal energy (and therefore information) is contained.

A value for $B_{eff}$ has been assumed between $B_{-10}$ and $B_{-20}$ (defined in Figs. 7 and 8) of the signal spectrum. The polyphase code obtained through sampling of an FM code keeps its salient features: same sidelobe levels and low Doppler sensitivity.

## B) EFFECT OF THE DISTORTION FACTOR $K_D$ AND OF PHASE DOPPLER SHIFT

The nonlinear frequency modulation law used is, as previously reported, the one at reference /7/ which is characterized by a distortion coefficient $K_D$(*) which varies in [0,1]:

$K_D = 0$, maximum distortion

$K_D = 1$, no distortion (linear modulation).

$K_D$ determines $\varphi$ (t) and therefore, in the polyphase code, the sequence of phases $\{\varphi_k\}$ and it has an impact on the peak-to-sidelobes ratios, the sidelobes distribution, the sensitivity to Doppler and range resolution due to the widening of the main lobe (see also Fig. 10).

Fig. 12 (curve "a") shows the peak-to-sidelobes ratio, function of $K_D$, at its worst, at the output of the matched filter in absence of Doppler shift. The percentage distribution of the sidelobes is given in table 1.

(*) Such coefficient is the same denoted by k in paragraph 6.

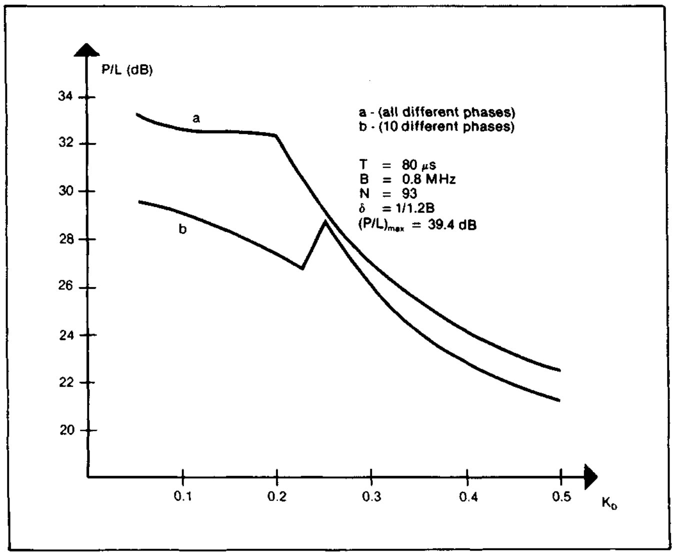


Fig. 12 - Peak-to-sidelobe ratio vs. $k_D$ for a NLFM digital code.

**TABLE 1**

| KD | 0.5 | 0.2 | 0.1 |
|---|---|---|---|
| P/L | 24.3 | 32.3 | 32.6 |
| % lobes < 40 dB | 53.3 | 63.3 | 61 |
| % lobes < -30 dB | 90 | 100 | 100 |
| % lobes < -25 dB | 99 | — | — |

Sidelobes distribution versus $K_D$; NLFM discrete code, with:

$f_D = 0$
N = 93
T = 80 μs
B = 0.75 MHz
$\delta$ = 1/(1.55 B)

Fig. 13 shows the ratio P/L as a function of Doppler frequency $f_D$ for different values of $K_D$ and for linear chirp, for comparison purposes. In the headings of Fig. 12 and following, the maximum of the peak-to-sidelobe ratio obtainable with a discrete phase code is reported for comparison purposes, i.e.:

$$(P/L)_{MAX} = 20 \log_{10} N$$

a value which is certainly present at both the right and left edges of the autocorrelation function.

As regards the presentation of the performance of the codes examined, we have here generally adopted the

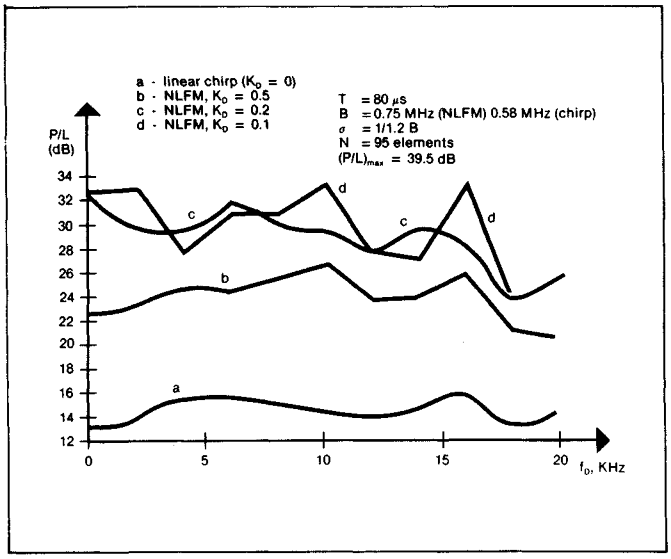


Fig. 13 - Peak-to-sidelobe ratio vs. Doppler frequency, for different $k_D$.

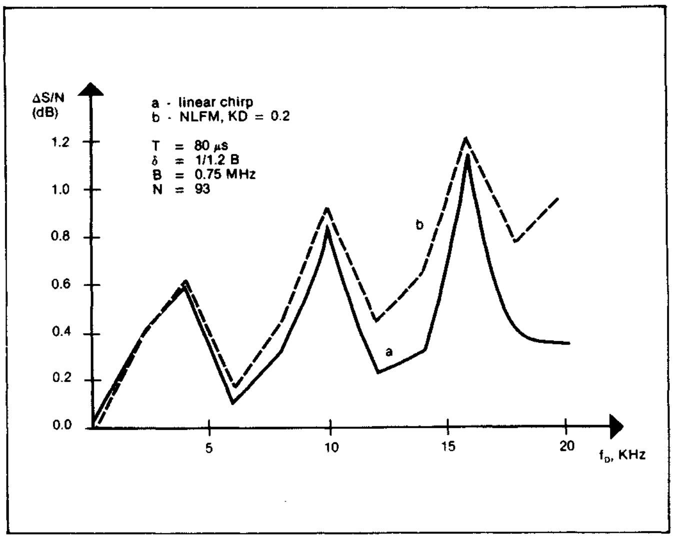


Fig. 14 - SNR mismatching loss due to Doppler frequency (NLFM digital code).

criteria to consider the peak-to-sidelobe ratio at its worst. Other criteria could be adopted, depending upon system requirements, (i.e. the quadratic average of the sidelobe levels). More complete information is given by the sidelobe level distribution, as in table 1.

The choice of coefficient $K_D$ must be based upon a trade-off between low sidelobes and moderate sensitivity to Doppler. The presence of a Doppler phase shift in the return echo, through signal mismatch, has an impact upon the response:

- peak attenuation (S/N loss),
- increase of sidelobe levels,
- time shifting of the response peak,
- response distortion around the peak.

In Fig. 14, the losses S/N (function of Doppler frequency) of the discrete chirp code obtained through an analog linear chirp, are compared with that obtained from the sampling of a nonlinear analog chirp having a distortion factor $K_D = 0.2$. The slight increase of losses in the case of nonlinear modulation is largely compensated for by the improved ratio P/L which (Fig. 13) is, on average ($K_D = 0.2$), 14 dB. In the discrete case, the peak shift is maintained proportional to the ratio $f_D/B$, which is typical of the analog chirp. Such shift, as $f_D$ is not known a priori, is reflected in an error on range amounting at any time to less than 3 $\delta$ when $f_D \leqslant 20$ KHz and B = 0.8 MHz.

The last effect considered is the presence of a "hump" on the main lobe at the matched filter output (see Fig. 15).

This distortion in the case of polyphase codes appears as a secondary peak close to the main one and would deteriorate range accuracy and discrimination; it is anyway present also in analog chirp codes /6/ although differently shaped.

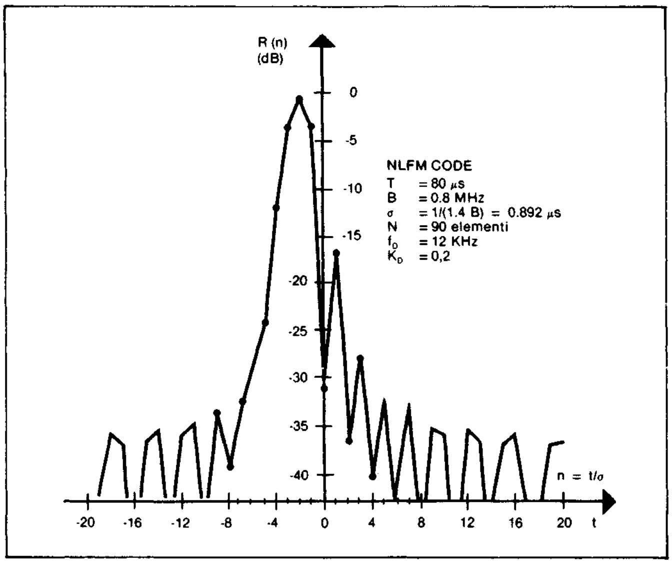


Fig. 15 - Output of a filter matched to a NLFM code, affected by Doppler shift.

## 8. Implementation problems

Putting into practice the previously analyzed polyphase codes, one must take into consideration the problems and the limitations which code generation and compression give way to when dealing with available technologies.

As for code generation, the RF must be phase modulated to obtain the desired phase shift at the transition from one sub-pulse to the other. The following problems arise:

— modulator complexity normally increases (*) with the number of distinct phase values (mod. $2\pi$);

— the effective phase values obtained are generally affected by implementation errors;

(*) For a number $2^M$ of equally spaced phases, the resulting complexity is almost proportional to M.

— corresponding to phase transition there is a spot where RF has a phase different from the steady-state value.

As regards code compression, based upon digital techniques, the following problems arise:

— lack of sync between echo starting point and sampling clock, with a resulting optimization of sampling frequency, that is of the ratio $\delta/T_c$;
— selection of the number of bits necessary for an accurate representation of signal and compression filter coefficients, taking into account its complexity.

The number of distinct phases is generally equal to half the number of code elements, because the phase sequence is usually symmetrical. It is most convenient to use the least number of distinct phase values, whereas there is no limitation to the phases themselves. To limit the number of distinct phases, the following method has been adopted: having synthesized a polyphase code, the values obtained have been replaced by near values properly selected so as to obtain a good approximation of the original code with a limited number of distinct phases.

In fig. 12, which has already been called up regarding the distortion factor, in addition to the curve indicated as (a) related to the case of all distinct phases, the graph for 10 distinct phases is also reported. It may be noted that the ratio P/L deteriorates all the more the lesser the number of distinct phases. To complete the analysis, consider the graphs in Fig. 16, where the ratio P/L is given as a function of the Doppler. Although no contraint exists a-priori in the choice of the distinct phase values, a uniform quantization of (0, $2\pi$) has been adopted.

In conclusion, a number of distinct phases equal to 16 (with a phase quantum equal to 22.5°), seems to be the minimum required so as not to deteriorate code performance by too large an extent and also seems to be a reasonable cost solution. The sequence of the phases for the 120 elements code is given in fig. 17.

As regards the errors in the effective transmitted phases, due to tolerances in the delay lines, to radar frequency agility or thermal noise, their effect amounts to a loss on the peak and a sidelobes degradation. The phase error has been modelled as a random, white, Gaussian process, with zero mean and assigned standard deviation.

In the case of 16 distinct phase values, errors having $\sigma \leqslant 4°$ do not influence, in any significant manner, the filter response. As regards the phase transient (where the phase may take any value), its duration is typically of a few percent of the sub-pulse duration. This problem is related to that of sampling in the receiver: assume, as an example, to select one sample for each sub-pulse, then for particular values of the target range the sampled values may be completely random. To obviate the problem, a shorter sampling interval is taken so as to have for each pulse, on average $(1+\epsilon)$ samples, where $\epsilon$ is opportunely tailored on the basis of the duration of the transient.

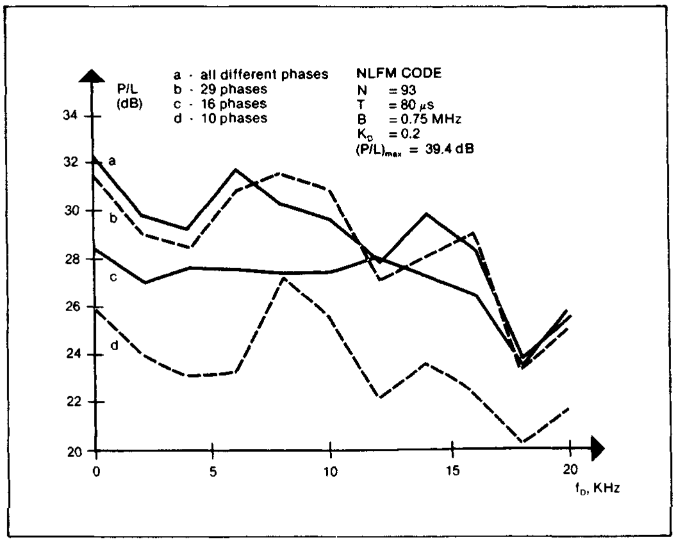


Fig. 16 · Peak-to-sidelobe ratio vs. Doppler frequency for different number of phases.

Fig. 17 · Sequence of phase values for a digital NLFM code with N = 120 elements.

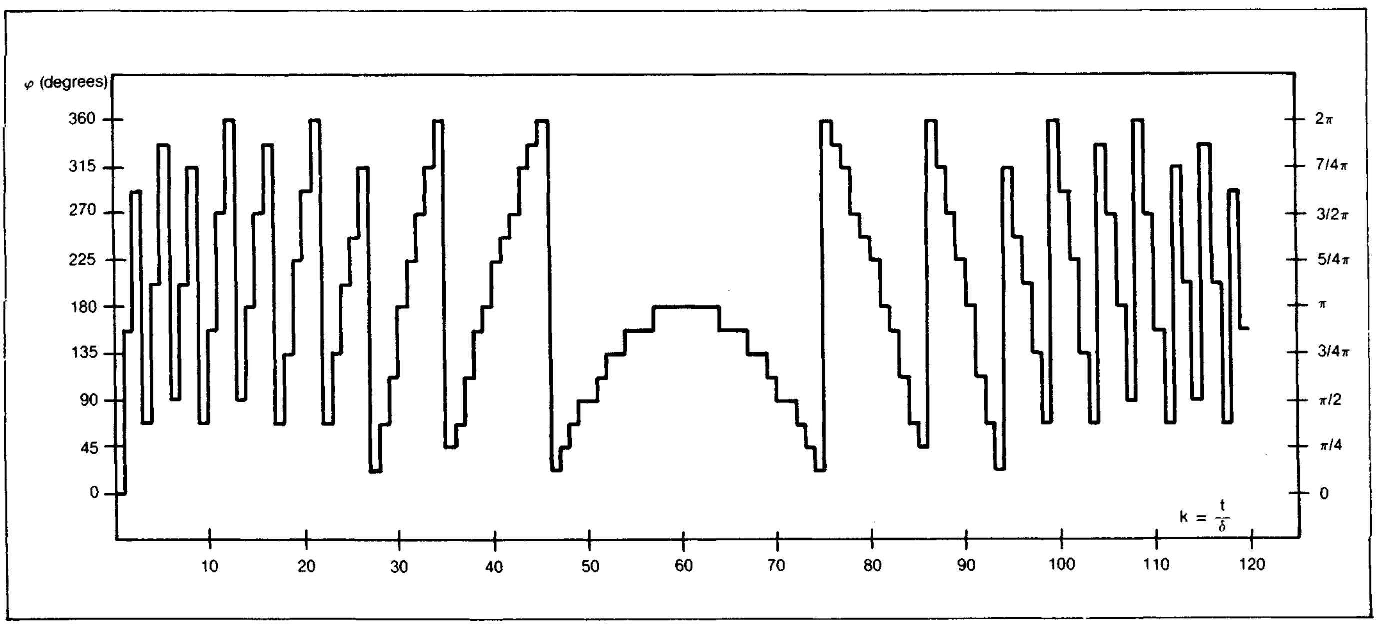

Through this technique, only a small percent of the samples will be mismatched with the correlation filter.

This phenomenon has been simulated by assigning a random value to a given fraction of the samples with a different number and position of the random elements. With a fraction of random samples between 1/20 and 1/40, the peak loss is less than 0.5 dB with a P/L ratio at all times greater than 24 dB, which stands for a degradation of the order of 4 or 5 dB, or less.

The results obtained are independent of the random element position in the group of samples.

A detailed evaluation of the signal quantization effect at the matched filter input and of the filter weights, is given in /11/.

The most significant result is that assuming that weights and signal have the same number of bits $n_B$ (inclusive of sign), when $n_B \leqslant 3$, a significant degradation of the peak-to-sidelobe ratio takes place, at least for codes having a relatively small number of elements.

Performance with $n_B = 4$ is generally satisfactory, so that such value may be considered a valid trade-off between cost and effectiveness. Further evaluations of the hardware complexity and available performances are given in /12/.

# 9. Conclusions

The discrete chirp codes are a family of waveforms with both the advantages of traditional chirp (i.e. high compression ratios, tolerance to Doppler shift) and that of making use of well tested processing techniques (MTI followed by a limiter and a matched filter) and of digital techniques utilising bi-phase codes (Barker and pseudonoise).

As a matter of fact, from an implementation viewpoint, discrete chirp may be seen as an extension of such codes.

## REFERENCES


[1] *Cook C.E., Bernfeld M. (1967)* — **Radar Signals** — Academic Press, New York

[2] *Frank R.L. (1963)* — **Polyphase codes with good non periodic correlation properties** — IEEE Trans. on Information Theory, Vol. IT-9, N. 1, 43 - 45.

[3] *Klauder J.R., Price A., Darlington S., Albersheim W.J. (1960)* — **The theory and design of Chirp Radars** — Bell System Technical Journal, Vol. 39, N. 4, 745 - 808

[4] *Rihaczek A.W. (1969)* — **Principles of high resolution radar** — Mc -Graw Hill, New York

[5] *Skolnik M.I. (1970)* — **Radar Handbook** — Mc - Graw Hill, New York

[6] *Berkowitz R.S. (1965)* — **Modern Radar** — John Wiley-Sons, New York

[7] *Millet R.E. (1970)* — **A matched-filter pulse-compression system using a non linear FM waveform** — IEEE Trans. on Aerospace and Electronic System, Vol AES-6, N.1, 73-78

[8] *Woodward P.M. (1953)* — **Probability and Information Theory, with applications to Radar** — Pergamon Press, New York

[9] *Galati G., Linardi V. (1974)* — **Analisi delle prestazioni in clutter di un radar navale...** — Selenia Technical Report (in Italian) RT-74153

[10] *Galati G., Fedele G. (1982)* — **Possibili forme d'onda per radar a lunga portata** — Selenia Technical Report (in Italian) RT-82054

[11] *Di Vito A., Farina A., Galati G., Studer F.A. (1983)* — **Progetto e valutazione della forma d'onda per un radar tridimensionale a grande portata** — Selenia Technical Report (in Italian) RT-83030

[12] *Bucciarelli T., Conti C., Fedele G., Strappaveccia S. (1984)* — **Design and implementation of a filter matched to a polyphase code in hard-limited radar channels** — Alta Frequenza, Vol. LIII, N. 5, 1984, 262-269

[13] *Orsini M. (1982)* — **Sintesi di segnali radar con funzione di ambiguità a bassi lobi laterali** — Thesis for the Degree in E.E. Università di Roma, Istituto di Comunicazioni Elettriche, Facoltà di Ingegneria.